

A non-spinning effective-one-body Hamiltonian for small-mass-ratio binaries in a quasi-circular orbit

Andrea Antonelli

Max Planck Institute for Gravitational Physics (Albert Einstein Institute, AEI), Potsdam

In collaboration with:

M. van de Meent, A. Buonanno, J. Steinhoff, J. Vines

*22nd Capra Meeting on
Radiation Reaction in General
Relativity*

@

CBPF, Rio de Janeiro



MAX-PLANCK-GESELLSCHAFT

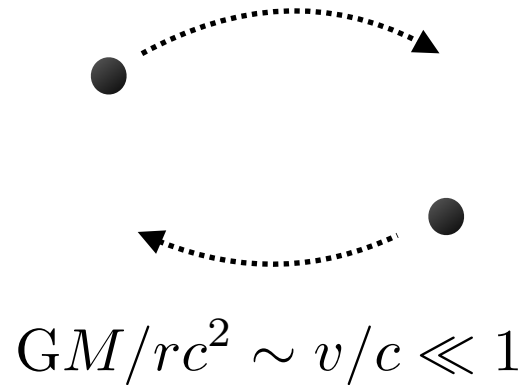
Plan of the talk

- Motivations.
- Review the construction of an effective-one-body (EOB) Hamiltonian with self-force information without unphysical divergences.
- Comparisons against numerical-relativity (NR) predictions.
- Conclusions.

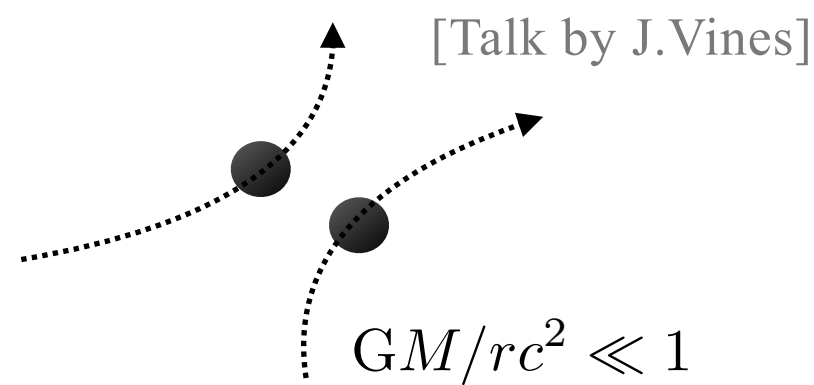
Motivation

Analytical approximations to solve general relativistic two-body problem: *Effective one body (EOB)*

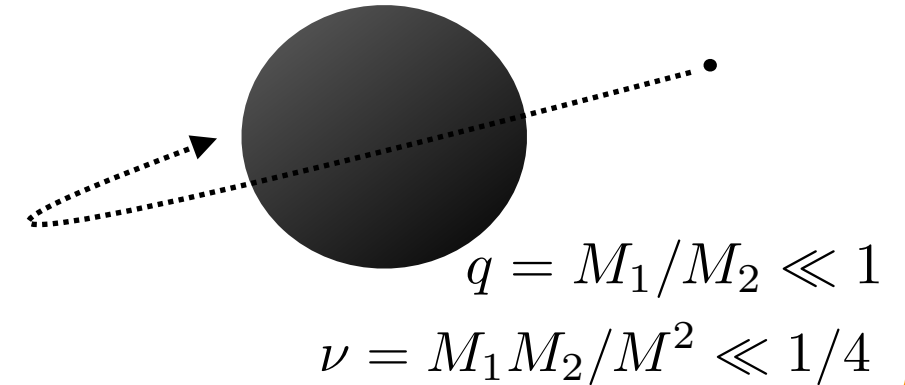
post-Newtonian (PN):



post-Minkowskian (PM):



small mass ratio (SMR):

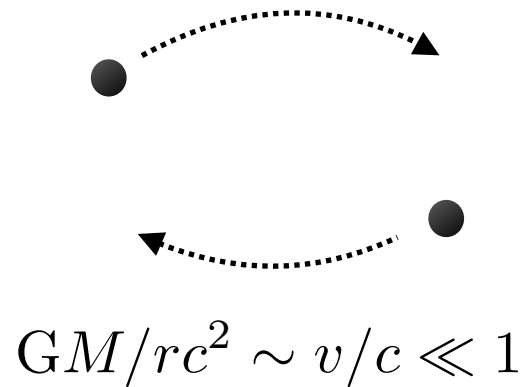


- Why is it important to include as much analytical information as possible in the EOB approach?

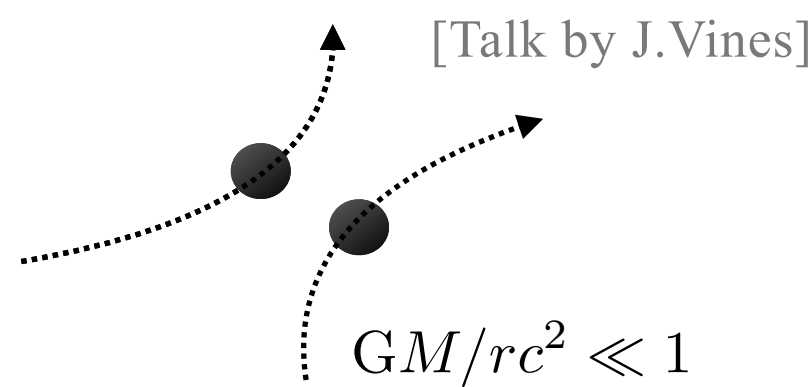
Motivation

Analytical approximations to solve general relativistic two-body problem: *Effective one body (EOB)*

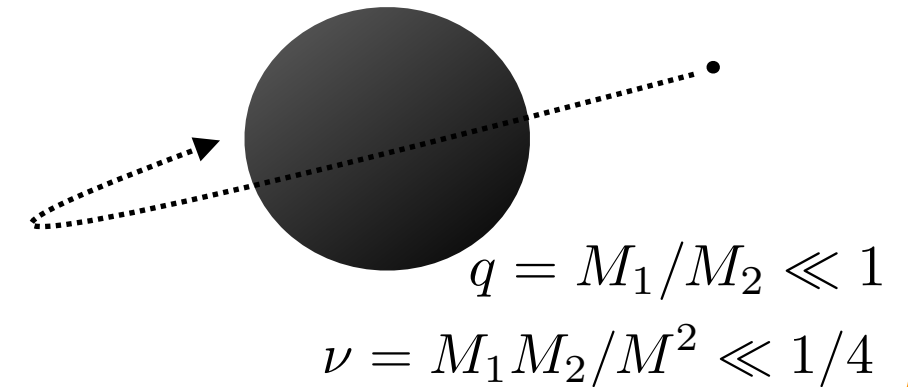
post-Newtonian (PN):



post-Minkowskian (PM):

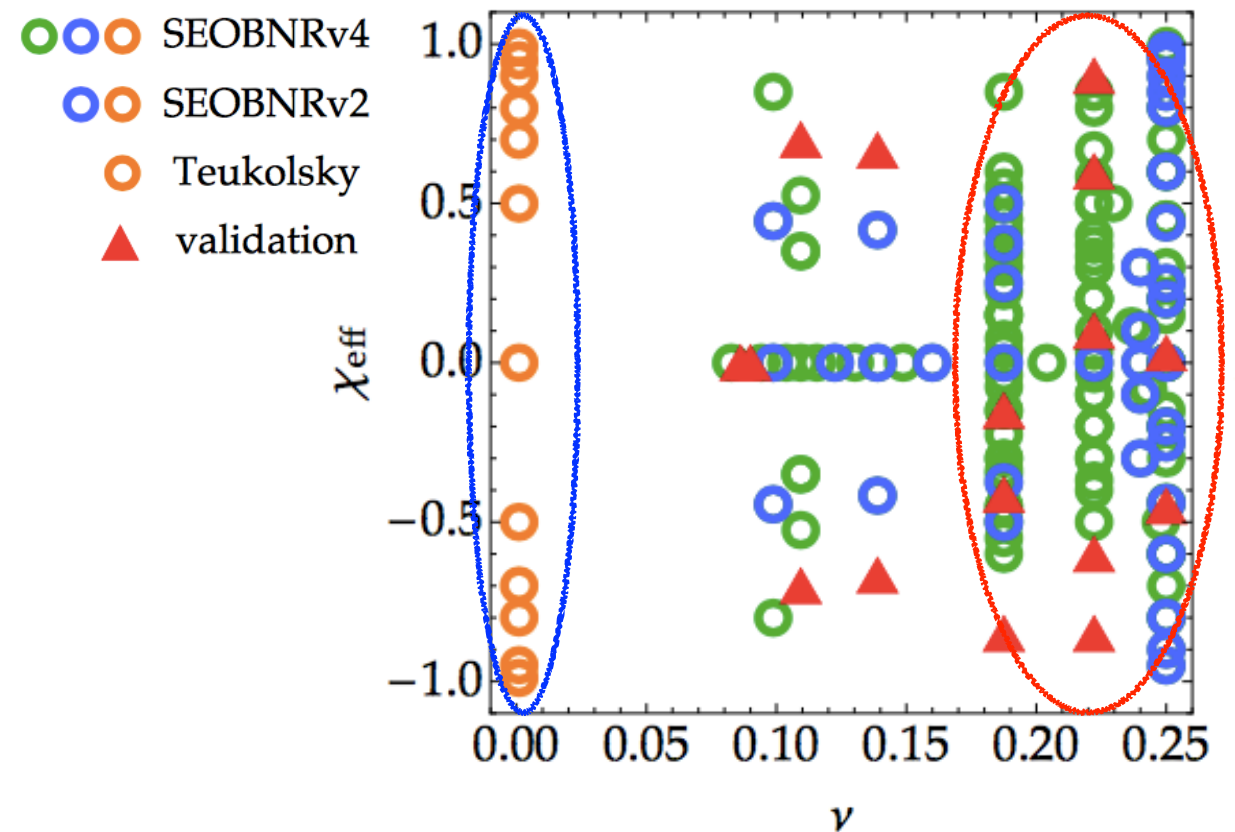


small mass ratio (SMR):



A concrete example:

- *SEOBNRv4* model [Bohè et al., 2016] is based on the PN approximation and calibrated to many **NR simulations** at high q 's ($1/4 \lesssim q = 1$) and solutions to the **Teukolsky** equations at small q 's ($q \lesssim 10^{-5}$) [Barausse et al. 2012, Taracchini et al., 2014].

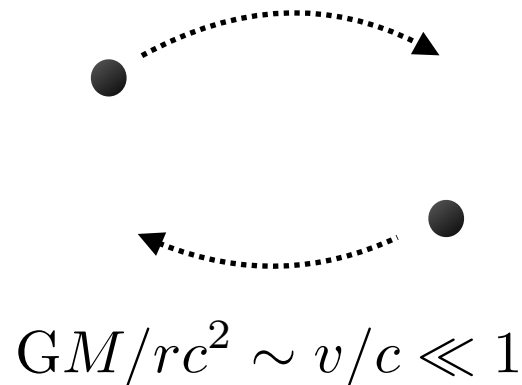


[Bohè et al. (2016)]

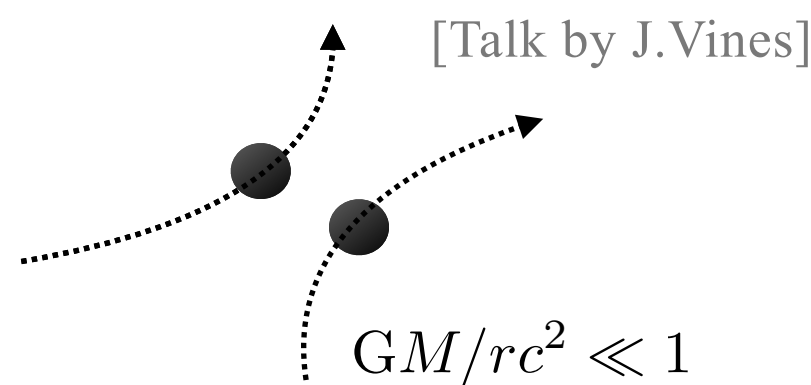
Motivation

Analytical approximations to solve general relativistic two-body problem: *Effective one body (EOB)*

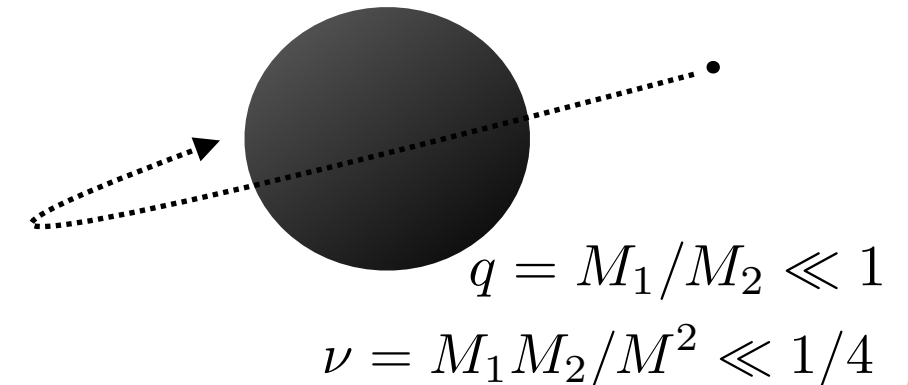
post-Newtonian (PN):



post-Minkowskian (PM):

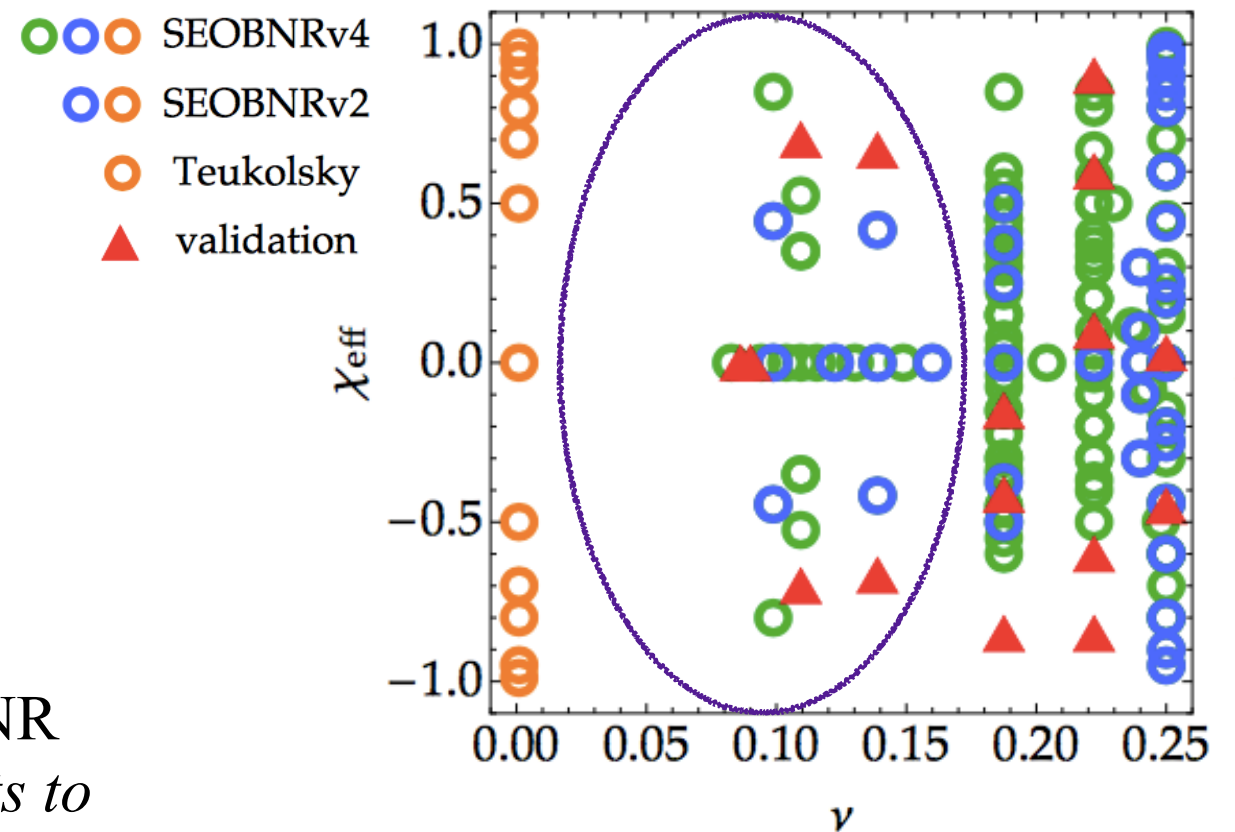


small mass ratio (SMR):



A concrete example:

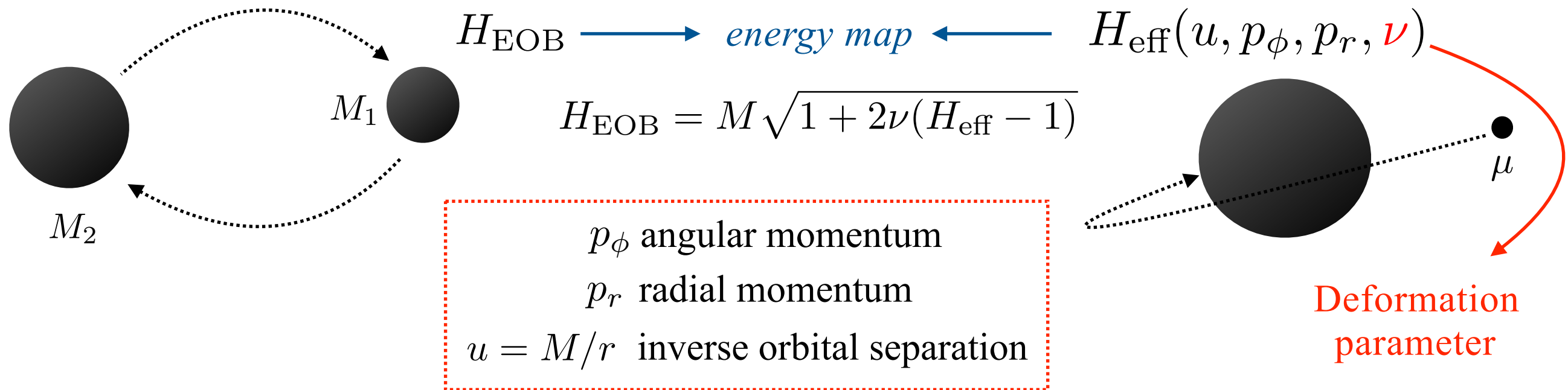
- *SEOBNRv4* model [Bohè et al., 2016] is based on the PN approximation and calibrated to many **NR simulations** at high q 's ($1/4 \lesssim q = 1$) and solutions to the **Teukolsky** equations at small q 's ($q \lesssim 10^{-5}$) [Barausse et al. 2012, Taracchini et al., 2014].
- Intermediate region ($1/10 \leq q \lesssim 1/4$): few NR simulations, *we need analytical improvements to avoid relying on interpolations.*



[Bohè et al. (2016)]

The effective-one-body formalism

- Real two-body problem solutions are mapped to an effective description of an effective mass in a geodesic around a *deformed* Schwarzschild (or Kerr) background:



- The *energy map* is the central resummation in EOB theory. In the standard (DJS) gauge, the effective Hamiltonian reads [Buonanno, Damour 1998 & Damour, Jaranowski, Schäfer, 2001,2014]:

$$\frac{H_{\text{eff}}}{\mu} = \sqrt{A(u, \nu) [1 + p_\phi^2 u^2 + A(u, \nu) D(u, \nu)^{-1} p_r^2 + Q_{\text{DJS}}(u, p_r, \nu)]}$$

Information from approximations to two-body problem in GR (so far, SMR information is added here)

Non-geodesic term starting at 3PN. Gauge choice: does not depend on angular momentum

Interface between EOB and SMR approximation

- Two approaches to include SF information into the EOB potentials:
 - 1) They can be informed by high-PN coefficients inspired by SF quantities: Detweiler redshift [Kavanagh, Bini, Damour, Geralico et al.], periastron advance [Le Tiec, Warburton et al.], self-tides [Dolan, Nagar, Akcay et al.].
 - 2) They can be specified semi-analytically. Example: SMR correction to the A potential via the Detweiler redshift $\Delta z(u)$ [Le Tiec et al. 2011, Barausse et al. 2011, Akcay et al. 2012]:

$$A(u, \nu) = 1 - 2u + \nu \left[\Delta z(u) \sqrt{1 - 3u} - u \left(1 + \frac{1 - 4u}{\sqrt{1 - 3u}} \right) \right]$$

Trouble at the LR!

- Divergence is a coordinate singularity due to the use of the DJS gauge [Akcay et al., 2012].
- The EOB binding energy for circular orbits scales as: $E_{\text{bind}}^{\text{EOB}} \propto A(u, \nu) p_{\phi}^2 \propto A(u, \nu) (1 - 3u)^{-1}$
- The SF binding energy scales as: $E_{\text{bind}}^{\text{SF}} \propto (1 - 3u)^{-3/2}$
- Matching SF and EOB binding energies, divergence leaks into the A potential, which then appears in the EOB Hamiltonian for *generic orbits*.

Alternative gauge

- In the DJS gauge, we are forced to have a p_ϕ^2 term in the geodesic part of the Hamiltonian.
- The post-Schwarzschild (PS) gauge, used for PM calculations in [Damour 2016, Damour 2017, Antonelli et al. 2019] can be used. The Hamiltonian in PS form is:

$$H_{\text{eff}} = \sqrt{H_S^2(u, p_\phi, p_r) + Q_{\text{PS}}(u, H_S, \nu)}$$

↓

*Test-body
limit*

↓

*Known @ 4PN and
3PM order*

Our strategy:

- Hamiltonian in this gauge depends on the new variable H_S .
- It is regular for generic orbits, but it diverges at the LR for circular orbits:

$$H_S = \sqrt{(1-2u)[1 + p_\phi^2 u^2 + (1-2u)p_r^2]} \xrightarrow[\substack{p_r = 0 \\ p_\phi^{\text{circ}} = \frac{1}{\sqrt{u(1-3u)}}}]{\substack{p_r = 0 \\ p_\phi^{\text{circ}} = \frac{1}{\sqrt{u(1-3u)}}}} H_S^{\text{circ}} = \frac{1-2u}{\sqrt{1-3u}}$$

- Key idea: push divergence of the EOB SMR Hamiltonian into H_S . In this way, we will recover the divergence *only* for circular orbits.

Circular-orbit self-force information in the post-Schwarzschild gauge

- We want to link the Detweiler redshift to the EOB effective potential. We split it as follows:

$$\Delta z(u) = \frac{1}{(1-3u)^{3/2}} \left[z_0(u) + z_1(u)\sqrt{1-3u} + z_2(u) \ln \left(\frac{(1-2u)^4}{(1-3u)^2} \right) \right]$$

- This motivates the following ansatz for the EOB SMR effective Hamiltonian:

$$H_{\text{eff}} = \sqrt{H_S^2(u, p_\phi, p_r) + Q_{\text{SMR}}(u, H_S, \nu)}$$

$$Q_{\text{SMR}}(u, H_S, \nu) = (1-2u)\nu [f_0(u)H_S^5 + f_1(u)H_S^2 + f_2(u)H_S^3 \ln H_S^4]$$

- We obtain the circular-orbit limit of the above at linear order in the mass ratio, in terms of the gauge-independent frequency x : $E_{\text{bind}}^{\text{EOB}}(x, \nu)$.
- The SF binding energy in the same limit, $E_{\text{bind}}^{\text{SF}}(x, z_{\text{SMR}}, \nu)$, is given by [Le Tiec et al., 2011].
- Matching the two at fixed frequency and imposing analyticity of f -functions, we get:

$$f_0 = \frac{1-3u}{(1-2u)^2} \left[\frac{z_0(u)}{(1-2u)^3} - \frac{1-4u}{(1-2u)^3} \right] \quad f_1 = \frac{z_1(u) - u}{(1-2u)^2} \quad f_2 = \frac{z_2(u)}{(1-2u)^3}$$

One way to add non-circular-orbit PN information

- Generic Hamiltonian in the PS gauge are known at 3PN order:

$$Q_{3\text{PN}}^{\text{PS}} = 3\nu u^2 Y + 5\nu u^3 + \left(3\nu - \frac{9}{4}\nu^2\right) u^2 Y^2 + \left(27\nu - \frac{23}{4}\nu^2\right) u^3 Y + \left(\frac{175}{3}\nu - \frac{41\pi^2}{32}\nu - \frac{7}{2}\nu^2\right) u^4$$

PN parameters:

$$Y \equiv (H_S^2 - 1) \sim \mathcal{O}(1/c^2)$$

$$u \equiv GM/rc^2$$

- They contain non-circular orbit information which is not captured by the matching of binding energies. We include extra PN information in a resummed term of the form:

$$Q_{\text{SMR-3PN}} = Q_{\text{SMR}} + \Delta Q_{\text{PN}}, \text{ with } \Delta Q_{\text{PN}} = \Delta Q_{\text{extra}} - \Delta Q_{\text{count}}$$

- The first term is fixed taking the difference between the EOB 3PN Hamiltonian in the PS gauge above and the PN limit of the EOB SMR Hamiltonian:

$$\Delta Q_{\text{extra}} = 3\nu u^2 Y + \left(3\nu - \frac{9}{4}\nu^2\right) u^2 Y^2 + 3\nu u^3 + \left(22\nu - \frac{23}{4}\nu^2\right) u^3 Y + \left(16\nu - \frac{7}{2}\nu^2\right) u^4$$

- The second term ensures that the above result does not contribute to the linear-in-mass-ratio circular-orbit binding energy.

$$\Delta Q_{\text{count}} = \nu(9u^3 Y^2 + 96u^4 Y + 112u^5)$$

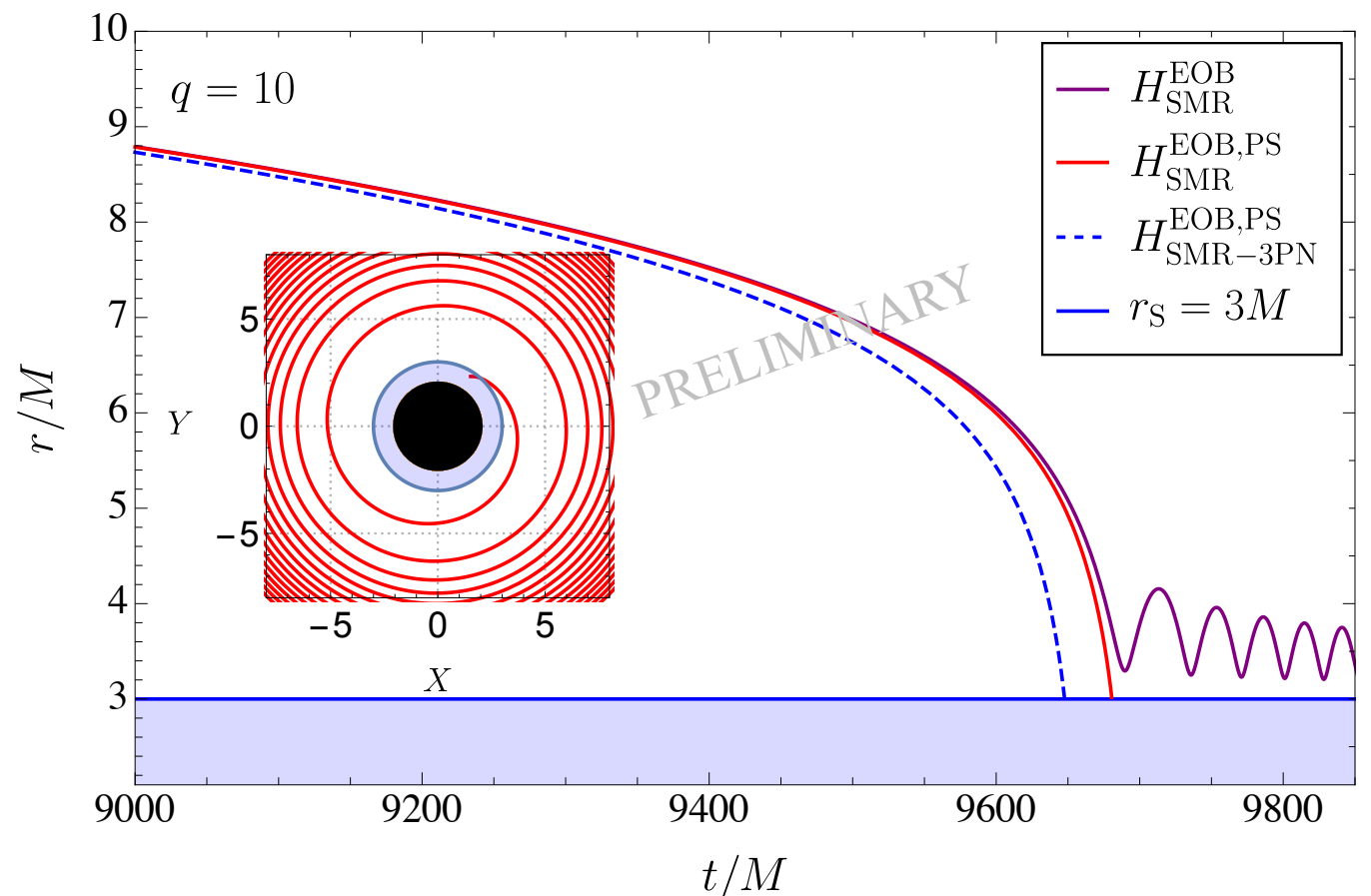
Evolutions of EOB Hamiltonians

- For a generic EOB Hamiltonian $H(r, p_\phi, p_{r_*})$, the Hamilton's equations are:

$$\frac{d\phi}{d\hat{t}} = \frac{\partial H}{\partial \hat{p}_\phi} \quad \frac{d\hat{r}}{d\hat{t}} = \frac{A(\hat{r})}{\sqrt{D(\hat{r})}} \frac{\partial H}{\partial \hat{p}_{r_*}}$$

$$\frac{d\hat{p}_\phi}{d\hat{t}} = \mathcal{F}_{\text{RR}} \quad \frac{d\hat{p}_{r_*}}{d\hat{t}} = -\frac{A(\hat{r})}{\sqrt{D(\hat{r})}} \frac{\partial H}{\partial \hat{r}} + \mathcal{F}_{\text{RR}} \frac{\hat{p}_{r_*}}{\hat{p}_\phi}$$

- The equations are augmented with a resummed “radiation reaction” flux from the SEOBNR family.
- We *do not* include NQC's or calibration terms for easier comparisons.
- Unphysical behaviour associated to the LR divergence in the DJS gauge is not there in the PS gauge.

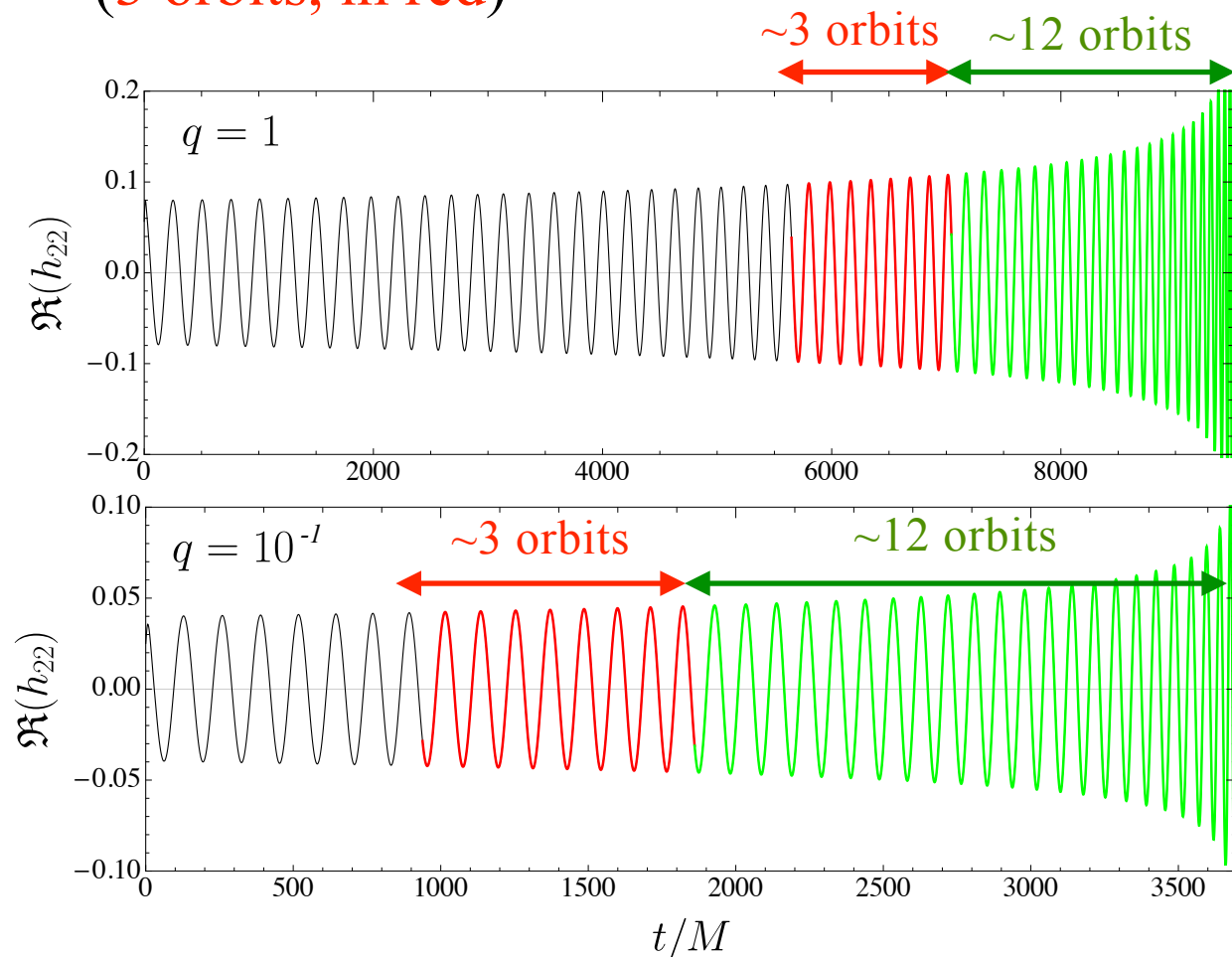


Phasing studies I: waveform alignment

- We want to assess the usefulness of SMR information. We perform a phasing study [for the leading (2,2) mode] between SMR and PN models against NR predictions.
- *Alignment procedure.* Minimise the following function for Δt and $\Delta\phi$ [Pan et al. 2011]:

$$\Xi(\Delta t, \Delta\phi) = \int_{t_1^{\text{alig}}}^{t_2^{\text{alig}}} [\phi_{\text{NR}}(t) - \phi_{\text{EOB}}(t + \Delta t) - \Delta\phi]^2 dt \quad \rightarrow \quad \begin{aligned} h_{22}^{\text{NR}} &= A_{\text{NR}}(t) \exp^{i\phi_{\text{NR}}(t)} \\ h_{22}^{\text{EOB}} &= A_{\text{EOB}}(t + \Delta t) \exp^{i\phi_{\text{EOB}}(t + \Delta t) + \Delta\phi} \end{aligned}$$

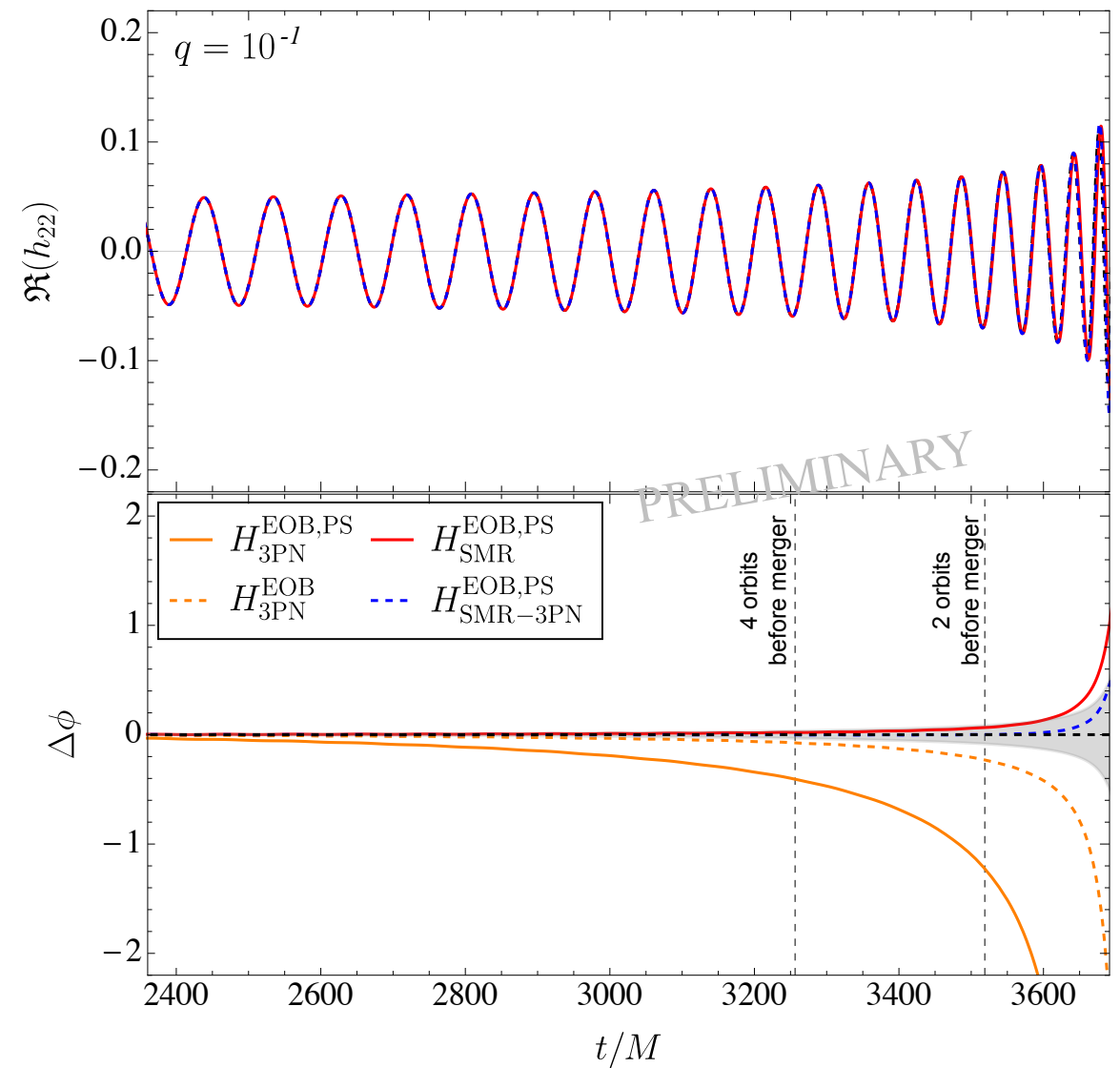
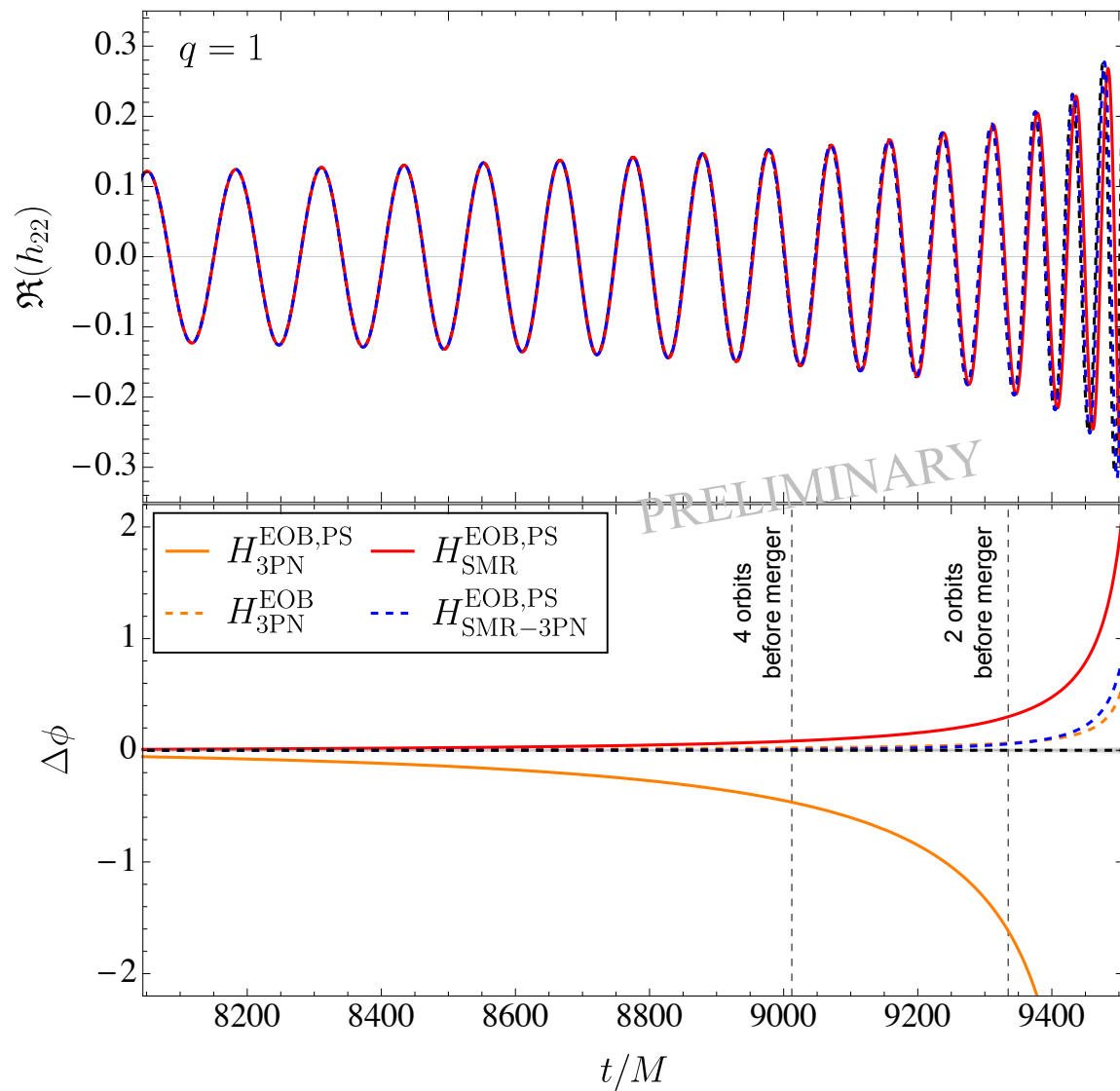
- We compare our waveforms to a set of 10 SXS simulations ($1/10 < q < 1$) [Boyle et al. 2019]. The alignment window encompasses the same number of GW cycles for each simulation (**3 orbits, in red**)



SXS ID:	q^{-1}	$N_{\text{orb}}^{\text{merg}}$	$t_{\text{in}}^{\text{alig}}$	$t_{\text{fin}}^{\text{alig}}$	t_{merg}
0180	1	28.18	5649	7044	9517
0169	2	15.68	29	1356	3728
0168	3	15.64	15	1254	3514
0167	4	15.59	0	1164	3326
0056	5	28.81	4634	5748	7864
0166	6	21.56	1819	2877	4891
0298	7	19.68	1164	2180	4142
0063	8	25.83	3028	4013	5956
0301	9	18.93	874	1824	3692
0303	10	19.27	938	1860	3691

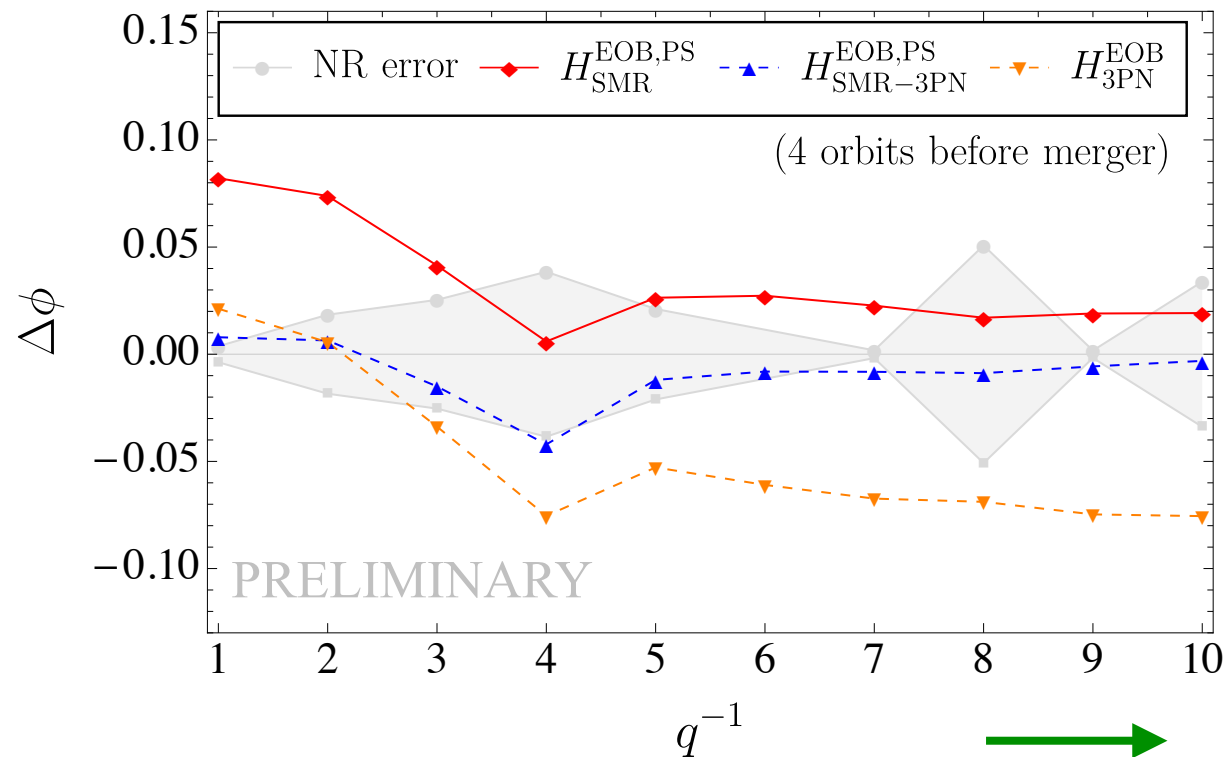
Phasing studies II: PN vs SMR

- Post-alignment results:

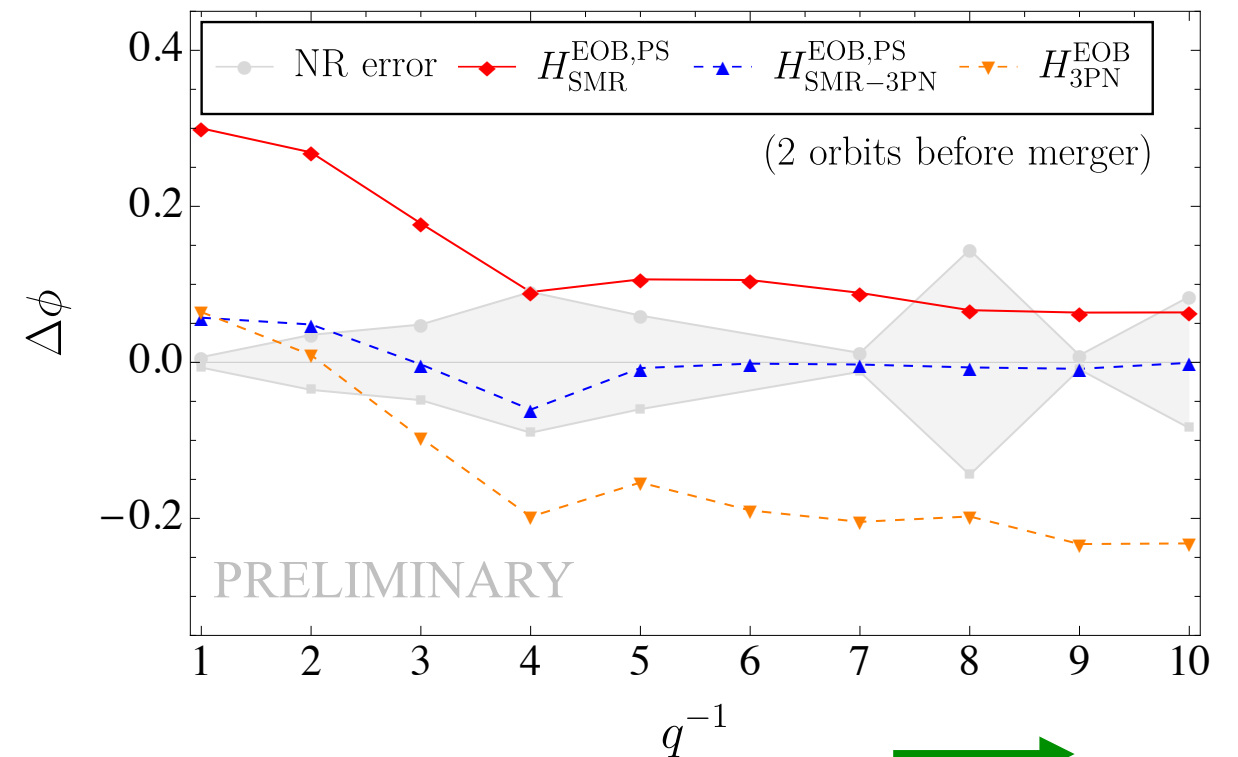


- *Top panel*: real part of the inspiral waveform for SMR models against the NR prediction.
- *Bottom panel*: accumulated de-phasing of SMR and PN models against NR, up to NR merger.
- Good agreement of SMR models up to few (NR) orbits to merger.

Phasing studies III: $\Delta\phi$ vs q



Stronger-field regime



Stronger-field regime

- We can look at the accumulated de-phasing few orbits before merger, and make comparisons across mass ratios.
- SMR-3PN model improves the modelling of the inspiral from $q \sim 1/3$ (when compared to the best-performing EOB-PN model).
- Results are robust against changes in the number of orbits before merger at which de-phasing is calculated and against changes in the time-alignment window.

Conclusions

Take-home points:

- We have a proof-of-principle EOBSMR model for non-spinning systems in a quasi-circular inspiraling orbit.
- SMR information shows great promise to improve the modelling of systems with $q < 1/3$ (when inserted in the EOB formalism).
- Self-force program is very useful for LIGO and 3G studies, not just for LISA.

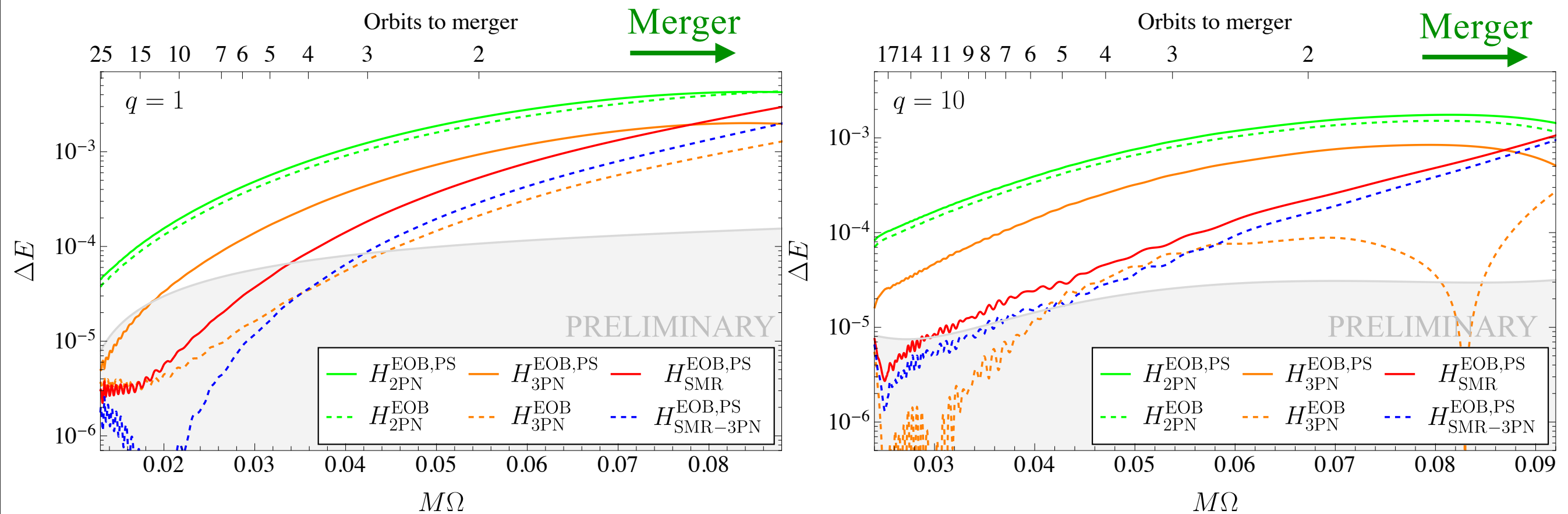
Outstanding issues:

- The non-geodesic function of the Hamiltonian in the PS gauge is not fully constrained. We need to include information from eccentric orbits to constrain its non-circular orbit sector.
[Remarks by Barry and Leor on SF scattering calculations]
- To be used, the model must be extended to include spins and merger and ringdown must be attached. Resulting inspiral-merger-ringdown models will need to be sped up.

Thank you!

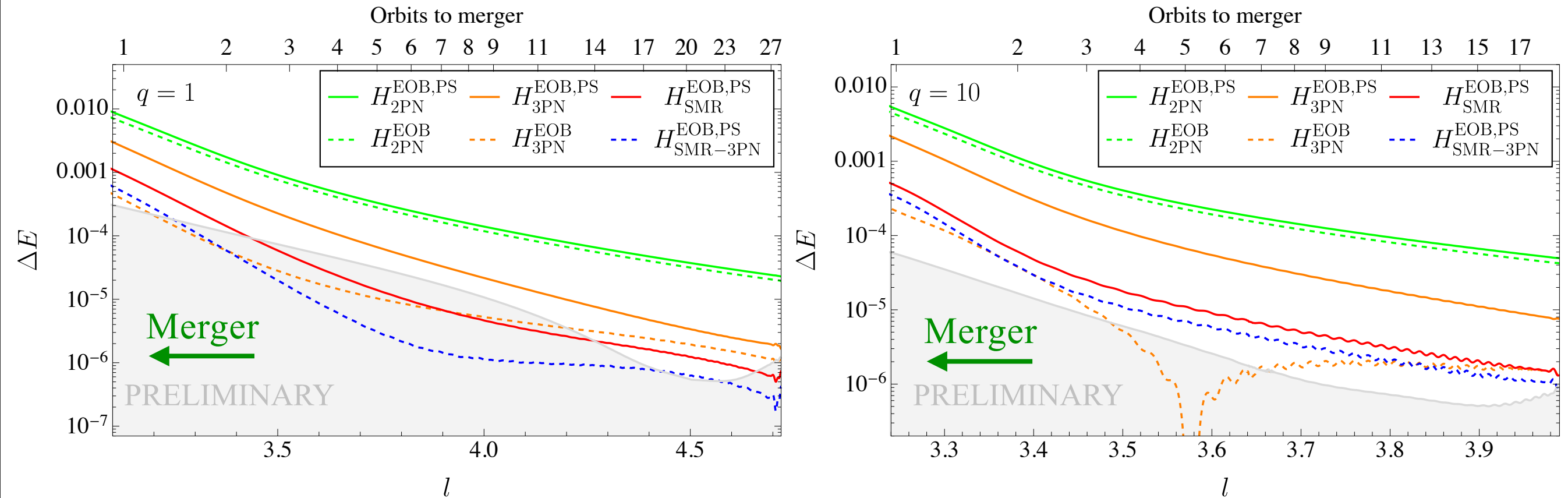
Extra slides

Energetics studies: E vs Ω



- The binding energy E vs frequency Ω curve is a gauge-invariant relation.
- For quasi-circular orbits, $E(\Omega)$ encapsulates the conservative dynamics. It can be used to compare analytical results to numerical predictions.
- SMR and SMR-3PN EOB Hamiltonians perform well against NR predictions and they are comparable to the 3PN EOB Hamiltonian in the DJS gauge.

Energetics comparisons: E vs l



- The binding energy E vs angular momentum l curve is a gauge-invariant relation.
- For quasi-circular orbits, $E(l)$ encapsulates the conservative dynamics and it can be used to compare analytical results to numerical predictions.
- SMR and SMR-3PN EOB Hamiltonians perform well against NR predictions and they are comparable to the 3PN EOB Hamiltonian in the DJS gauge.

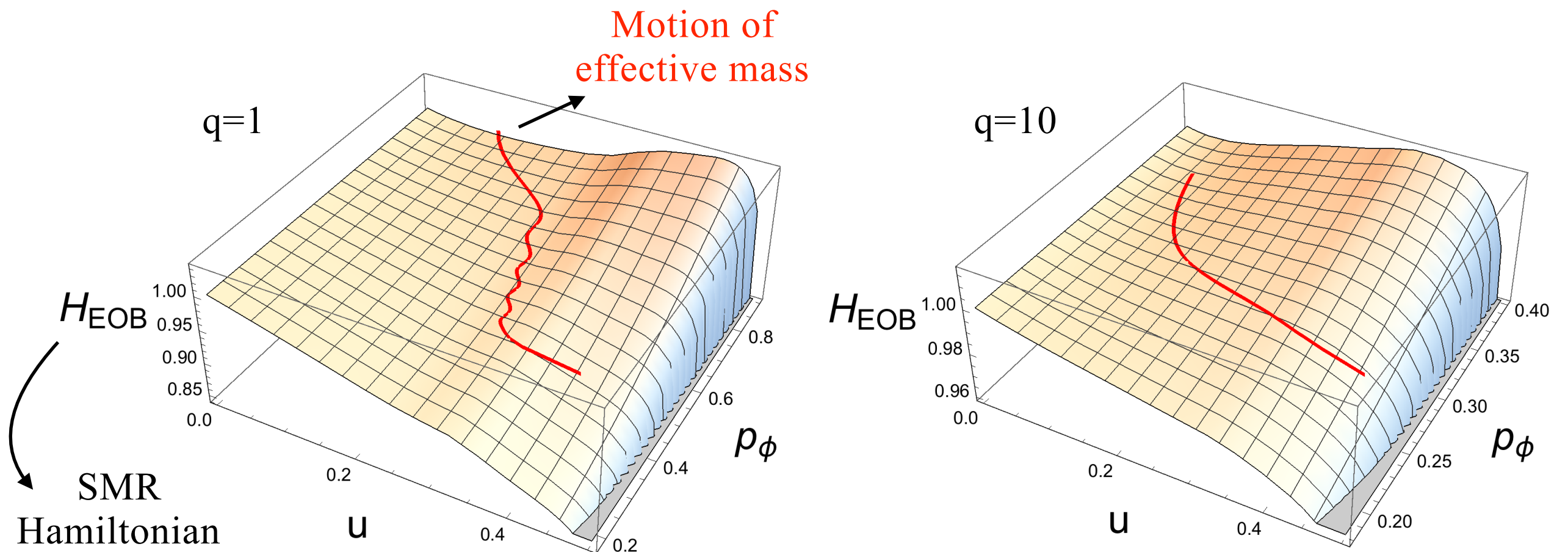
Residual eccentricity in comparable-mass systems

- In principle, an H_S^3 power in the Hamiltonian ansatz is enough to capture the global divergence in the redshift.

$$\Delta z(u) = \frac{1}{(1-3u)^{3/2}} \left[z_0(u) + z_1(u) \sqrt{1-3u} + z_2(u) \ln \left(\frac{(1-2u)^4}{(1-3u)^2} \right) \right]$$

↪ Scales as H_S^3

- The SMR Hamiltonian with H_S^3 contains bumps near the LR which result, for comparable-mass systems, in seemingly eccentric behaviour:



Residual eccentricity in comparable-mass systems

- In principle, an H_S^3 power in the Hamiltonian ansatz is enough to capture the global divergence in the redshift.

$$\Delta z(u) = \frac{1}{(1-3u)^{3/2}} \left[z_0(u) + z_1(u) \sqrt{1-3u} + z_2(u) \ln \left(\frac{(1-2u)^4}{(1-3u)^2} \right) \right]$$


 Scales as H_S^3

- With H_S^5 , the only factor changing in the Hamiltonian is the following:

$$f_0 = \frac{1-3u}{(1-2u)^2} \left[\frac{z_0(u)}{(1-2u)^3} - \frac{1-4u}{(1-2u)^3} \right] \quad f_1 = \frac{z_1(u) - u}{(1-2u)^2} \quad f_2 = \frac{z_2(u)}{(1-2u)^3}$$


 We introduce this factor

- Both H_S^3 and H_S^5 are valid solutions, because the Q -function is not fixed for generic orbits.
- We choose H_S^5 because it is the simplest modification to the H_S^3 ansatz that:
 - 1) maintains the Hamiltonian real after the Schwarzschild light ring.
 - 2) smooths out the otherwise-present bumps in the EOB Hamiltonian near the LR.